



ALMA MATER STUDIORUM
UNIVERSITÀ DI BOLOGNA

ARCHIVIO ISTITUZIONALE
DELLA RICERCA

Alma Mater Studiorum Università di Bologna Archivio istituzionale della ricerca

Targeting Helicobacter pylori urease activity and maturation: In-cell high-throughput approach for drug discovery

This is the final peer-reviewed author's accepted manuscript (postprint) of the following publication:

Published Version:

Targeting Helicobacter pylori urease activity and maturation: In-cell high-throughput approach for drug discovery / Tarsia, Cinzia; Danielli, Alberto; Florini, Francesca; Cinelli, Paolo; Ciurli, Stefano; Zambelli, Barbara*. - In: BIOCHIMICA ET BIOPHYSICA ACTA-GENERAL SUBJECTS. - ISSN 0304-4165. - STAMPA. - 1862:10(2018), pp. 2245-2253. [10.1016/j.bbagen.2018.07.020]

Availability:

This version is available at: <https://hdl.handle.net/11585/644152> since: 2018-09-21

Published:

DOI: <http://doi.org/10.1016/j.bbagen.2018.07.020>

Terms of use:

Some rights reserved. The terms and conditions for the reuse of this version of the manuscript are specified in the publishing policy. For all terms of use and more information see the publisher's website.

This item was downloaded from IRIS Università di Bologna (<https://cris.unibo.it/>).
When citing, please refer to the published version.

(Article begins on next page)

This is the final peer-reviewed accepted manuscript of:

C. Tarsia, A. Danielli, F. Florini, P. Cinelli, S. Ciurli, B. Zambelli; "Targeting Helicobacter pylori urease activity and maturation: In-cell high-throughput approach for drug discovery" (2018) *Biochim. Biophys. Acta Gen. Subj.* 1862(10):2245-2253. doi: 10.1016/j.bbagen.2018.07.020

The final published version is available online at:
[<https://doi.org/10.1016/j.bbagen.2018.07.020>]

Rights / License:

The terms and conditions for the reuse of this version of the manuscript are specified in the publishing policy. For all terms of use and more information see the publisher's website.

This item was downloaded from IRIS Università di Bologna (<https://cris.unibo.it/>)

When citing, please refer to the published version.

1
2
3
4
5
6
7
8
9
10
11
12
13
14
15
16
17
18
19
20
21
22
23
24
25
26
27
28
29
30
31
32
33
34
35
36
37
38
39
40
41
42
43
44
45
46
47
48
49
50
51
52
53
54
55
56
57
58
59
60
61
62
63
64
65

Targeting *Helicobacter pylori* urease activity and maturation: in-cell high-throughput approach for drug discovery

Cinzia Tarsia[#], Alberto Danielli[#], Francesca Florini, Paolo Cinelli, Stefano Ciurli, Barbara Zambelli*

Department of Pharmacy and Biotechnology, University of Bologna, Viale G. Fanin 40, 40127 Bologna (Italy)

[*barbara.zambelli@unibo.it](mailto:barbara.zambelli@unibo.it)

[#]CT and AD contributed equally to this work

1
2
3
4
5
6
7
8
9
10
11
12
13
14
15
16
17
18
19
20
21
22
23
24
25
26
27
28
29
30
31
32
33
34
35
36
37
38
39
40
41
42
43
44
45
46
47
48
49
50
51
52
53
54
55
56
57
58
59
60
61
62
63
64
65

Abstract

Background. *Helicobacter pylori* is a bacterium strongly associated with gastric cancer. It thrives in the acidic environment of the gastric niche of large portions of the human population using a unique adaptive mechanism that involves the catalytic activity of the nickel-dependent enzyme urease. Targeting urease represents a key strategy for drug design and *H. pylori* eradication.

Method. Here, we describe a novel method to screen, directly in the cellular environment, urease inhibitors. A ureolytic *Escherichia coli* strain was engineered by cloning the entire urease operon in an expression plasmid and used to test in-cell urease inhibition with a high-throughput colorimetric assay. A two-plasmid system was further developed to evaluate the ability of small peptides to block the protein interactions that lead to urease maturation.

Results. The developed assay is a robust cellular model to test, directly in the cell environment, urease inhibitors. The efficacy of a co-expressed peptide to affect the interaction between UreF and UreD, two accessory proteins necessary for urease activation, was observed. This event involves a process that occurs through folding upon binding, pointing to the importance of intrinsically disordered hot spots in protein interfaces.

Conclusions. The developed system allows the concomitant screening of a large number of drug candidates that interfere with the urease activity both at the level of the enzyme catalysis and maturation.

General significance. As inhibition of urease has the potential of being a global antibacterial strategy for a large number of infections, this work paves the way for the development of new candidates for antibacterial drugs.

1
2
3
4
5
6
7
8
9
10
11
12
13
14
15
16
17
18
19
20
21
22
23
24
25
26
27
28
29
30
31
32
33
34
35
36
37
38
39
40
41
42
43
44
45
46
47
48
49
50
51
52
53
54
55
56
57
58
59
60
61
62
63
64
65

Keywords: urease; nickel delivery; drug screening; protein-protein interactions; enzyme

inhibitors; *Helicobacter pylori*

1. Introduction

Helicobacter pylori is a widespread Gram-negative bacterium infecting the stomach of millions of people every year, up to 50 % of adults and reaching 80 – 90 % in developing countries [1]. After colonization, untreated *H. pylori* infections persist, often asymptotically, for the entire life-span of the host, because of the inability of the human immune response to efficiently counteract the bacterium. The infection causes chronic inflammation of the gastric mucosa, which can slowly progress to gastric adenocarcinoma or mucosa-associated lymphoid tissue (MALT) lymphoma. Accordingly, in 1994 the WHO classified *H. pylori*, first and unique among all bacteria, as a class I carcinogen [2] and reconfirmed this classification in 2012 [3]. Several meta-analyses pointed out that eradication of *H. pylori* at the population level would have beneficial effects, such as reduction in gastric cancer incidence, peptic ulcer development, dyspepsia symptoms, and anemia occurrence[4]. In addition, *H. pylori* eradication causes complete regression in 60%-80% of already established MALT lymphomas [5]. Therefore, the Gastric Cancer Consensus Conference boldly recommended population-based screening and treatment for *H. pylori* to prevent gastric cancer [6].

Nonetheless, treatment efficacy remains a major concern. The standard first-line therapy to eradicate *H. pylori*, using a combination of three different antibiotics, fails in 20% of the cases because of antibiotic resistance, leading to an increasing number of infected individuals harboring resistant bacteria. Indeed, in 2017 WHO included *H. pylori* in the list of antibiotic-resistant bacteria for which antibiotic development is a global priority [7].

To survive inside the very acidic environment of the gastric niche, *H. pylori* has created a unique adaptive mechanism relying on the Ni(II)-dependent enzyme urease, which catalyzes the rapid hydrolysis of urea to produce ammonia and carbamate. The latter spontaneously hydrolyzes, generating an increase of pH that buffers the micro-environment surrounding the

1
2
3
4
5
6
7
8
9
10
11
12
13
14
15
16
17
18
19
20
21
22
23
24
25
26
27
28
29
30
31
32
33
34
35
36
37
38
39
40
41
42
43
44
45
46
47
48
49
50
51
52
53
54
55
56
57
58
59
60
61
62
63
64
65

bacterium [8,9]. Indeed, urease-deficient *H. pylori* strains cannot colonize the stomach niche of mice [10]. Similarly, mutants that can synthesize the apo-urease but are unable to incorporate Ni(II) into its active site are unable to colonize the gastric mucosa, thereby highlighting a link between Ni(II) activation of urease and host colonization [11]. Interestingly, standard therapy reaches significantly higher eradication rates if a nickel-free diet is maintained by infected patients, suggesting that the reduction of urease activity could increase the bacterial susceptibility to antibiotics [12]. Higher eukaryotes do not produce urease, nor other nickel enzymes, rendering urease activity an attractive target for the development of alternative and specific antibacterial strategies to overcome *H. pylori* gastric infection.

Urease proteins are generally heteropolymeric proteins with a quaternary structure $(\alpha\beta\gamma)_3$ [8]. In bacteria of the genus *Helicobacter* the trimer is of the type $(\alpha\beta)_3$, with the β subunits corresponding to the fused β and γ subunits normally found in other bacteria. The protein also presents a higher level of oligomerization, with an $[(\alpha\beta)_3]_4$ quaternary structure. The activity of urease relies on the presence of a binuclear active site containing two Ni(II) ions, bridged by the carboxylate group of a carbamylated lysine, essential to maintain the ions at the right distance for the catalysis, and by a hydroxide ion, the nucleophile of the hydrolysis reaction [8,13]. This architecture, always present in the α subunit, is fully conserved in all known urease structures. Nickel incorporation into the active site of urease occurs post-translationally during enzyme maturation, and requires the assistance of the accessory proteins UreD, UreF, UreG and UreE, expressed from genes belonging to the urease operon [14]. UreE is a homodimeric protein responsible for Ni(II) delivery into the urease active site, while UreG is an intrinsically disordered GTPase that energizes the process of urease maturation [15]. In solution, UreE and UreG form a complex UreE₂-UreG₂, whose structure

1
2
3
4
5
6
7
8
9
10
11
12
13
14
15
16
17
18
19
20
21
22
23
24
25
26
27
28
29
30
31
32
33
34
35
36
37
38
39
40
41
42
43
44
45
46
47
48
49
50
51
52
53
54
55
56
57
58
59
60
61
62
63
64
65

90 has been obtained with molecular modeling and protein docking [16], and subsequently
91 confirmed by NMR [14]. The crystal structure of UreD₂-UreF₂-UreG₂ was reported [17], this
92 larger complex being a multiprotein composite chaperone that pre-activates apo-urease
93 before Ni(II) incorporation, a modification necessary for the enzyme to build up a correct
94 active site.

95 In an attempt to provide a model system to test new antibacterial molecules that target *H.*
96 *pylori*, we engineered a ureolytic *E. coli* strain to screen urease inhibitors by means of an in-
97 cell high-throughput colorimetric assay. In addition, we set up a two-plasmid system to
98 evaluate the ability of peptide sequences to block the protein-protein interactions (PPIs)
99 among the accessory proteins that lead to enzyme maturation. This method was used
100 successfully to screen the inhibition activity of a co-expressed peptide.

1
2
3
102
5
6
103
8
104
10
11
105
12
13
106
15
107
17
18
108
20
109
22
110
23
111
24
112
25
113
27
114
28
115
29
116
30
117
31
118
32
119
33
120
34
121
35
122
36
123
37
124
38
125
39
40
41
42
43
44
45
46
47
48
49
50
51
52
53
54
55
56
57
58
59
60
61
62
63
64
65

2. Experimental section

2.1. Gene cloning and site-directed mutagenesis

A scheme of the cloning strategy used in this work is presented in Figure 1SI. A list of the plasmids used in this work, with a short description, and of the oligonucleotide sequences needed for the molecular biology setup is reported in Table SI1 and SI2 respectively. Briefly, the *pGEM-ureOP* plasmid, carrying the *H. pylori* strain G27 urease operon (National Center for Biotechnology Information code NC_011333.1) [18], was used as PCR template for amplifying the *ureABIE* portion of the urease operon, containing the structural urease genes *ureA* and *ureB*, the urea membrane transporter gene *ureI* and the metallo-chaperone gene *ureE*, using *ureOP_F* and *ureE_R*. The purified PCR product was ligated (T4 DNA ligase) into the *pGEM-T* Easy vector according to the manufacturer instructions. The resulting construct (*pGEM-ureABIE*) was purified, analyzed by restriction analysis, and sequenced at the 5' and 3' ends to verify the correct insertion of the partial operon. Site directed mutagenesis was performed on *pGEM-ureOP* to create a urease operon containing a truncated version of *ureF* gene, lacking the C-terminal 21 residues (here called *pGEM-ureOP $\Delta\alpha$ F*), by amplifying the entire plasmid using the mutagenic primers *ureF_STOP* and *ureF_Blg_R*. Using *pGEM-ureOP* as a template, *ureF* gene was amplified using *ureF_Xho_F* and *ureF_Hind_R* oligos. The gene was double-digested using *XhoI* and *HindIII* restriction enzymes and eventually cloned into the *pBAD/His-Myc* vector (ThermoFisher) digested with the same restriction enzymes. This construct was used as template for amplifying the *araC-pBAD-ureF* portion, containing the *ureF* gene downstream to the arabinose promoter, using the *pBAD_Xba_F* and *pBAD_BspHI_R* oligonucleotides. Similarly, the *pXG-0* vector [19] was used as a template for a PCR reaction using *HSC_Xba_F* and *HSC_BspH_R* oligonucleotides, generating a DNA fragment containing the *pSC101* origin of replication and the

1
2
3
126 chloramphenicol resistance gene. The *pBAD-ureF* and *pXG-0* PCR products were double-
5
127 digested using XbaI and BspHI and ligated to give the *pXG0-pBAD-ureF* construct, containing
6
8
128 the *ureF* gene under the control of the arabinose promoter, and with the pSC101 origin of
10
11
129 replication and the chloramphenicol acetyl transferase gene. This construct was then digested
12
13
130 using XhoI and HindIII restriction enzymes and the gene coding for the 21-residues C-
15
16
131 terminal α -helix of UreF (αF), obtained by annealing the αF_{Xho_F} and αF_{Hind_R} oligos
17
18
132 was cloned in under the control of arabinose promoter.
20
21
133 Finally, the αF coding gene, deriving from the annealing of αF_{Nco_F} and αF_{Bam_R} oligos
22
23
134 was cloned in frame with the GB1 gene in the *pETM-12* [20] previously digested with NcoI
25
26
135 and BamHI. Subsequently, the *GB1- αF* gene was amplified using the *GB1 αF -Xho_F* and
27
28
136 *GB1 αF -Hind_R*, double digested with XhoI and HindIII and cloned into the *pXG0-pBAD*
30
31
137 vector, to obtain *pXG0-pBAD-GB1 αF* plasmid expressing GB1 protein fused with αF .
32
33

138 35 139 **2.2. In-cell urease activity test** 37

38
140 TOP10 cells harboring *pGEM-ureOP* plasmid or its derivatives, co-transformed, if needed,
40
141 with *pXG0-pBAD-ureF*, *pXG0-pBAD- αF* or *pXG0-pBAD-GB1 αF* were pre-cultured at 37 °C in
42
43
142 1 mL of lysogeny broth (LB) containing 50 μ g/mL of carbenicillin (Cb), and, for the double
45
46
143 transformant, 25 μ g/mL of chloramphenicol (Cm). After 16 hours, 200 μ L were used to
47
48
144 inoculate 2 mL of M9 medium (1 liter contained 6 g of Na₂HPO₄, 3 g of KH₂PO₄, 0.5 g of
50
51
145 NaCl, 1.25 g of (NH₄)₂SO₄, 0.246 g of MgSO₄, 4 g of glucose) containing the appropriate
52
53
146 antibiotics and 10 μ g/L of cresol red pH indicator. When OD600 reached 0.7-0.9, 100 μ L of
54
55
147 each culture were inoculated in 96-well plates with the appropriate concentration of urea, and
57
58
148 with or without 0.5% arabinose or the appropriate inhibitor concentrations. Immediately before
59
60
149 running the experiment, NiSO₄ was added to each culture. In each well, 50 μ L of mineral oil
62
63
64
65

1
2
3
4
5
6
7
8
9
10
11
12
13
14
15
16
17
18
19
20
21
22
23
24
25
26
27
28
29
30
31
32
33
34
35
36
37
38
39
40
41
42
43
44
45
46
47
48
49
50
51
52
53
54
55
56
57
58
59
60
61
62
63
64
65

were added to prevent medium evaporation during the culture. The color change of cresol red indicator was monitored over time spectrophotometrically in a multi-plate reader, measuring the absorption at 430 nm and at 580 nm.

1
2
3
154
5
6
155
8
156
10
11
157
12
13
158
15
159
17
18
19
20
21
22
23
24
25
26
27
28
29
30
31
32
33
34
35
36
37
38
39
40
41
42
43
44
45
160
47
161
49
50
162
51
163
52
164
53
165
54
55
166
57
58
167
59
60
168
62
63
64
65

3. Results

3.1. In-cell test of urease activity

The 6,500 bp urease operon[8] (*ureOP*) coding for both the structural and accessory genes of the *Helicobacter pylori* enzyme (Figure 1A) was cloned in an expression vector to yield *pGEM-ureOP* (Figure 1B and Figure 1SI) and used to express the holo-urease enzyme in recombinant BL21(DE3) *E. coli*, as previously described [18].

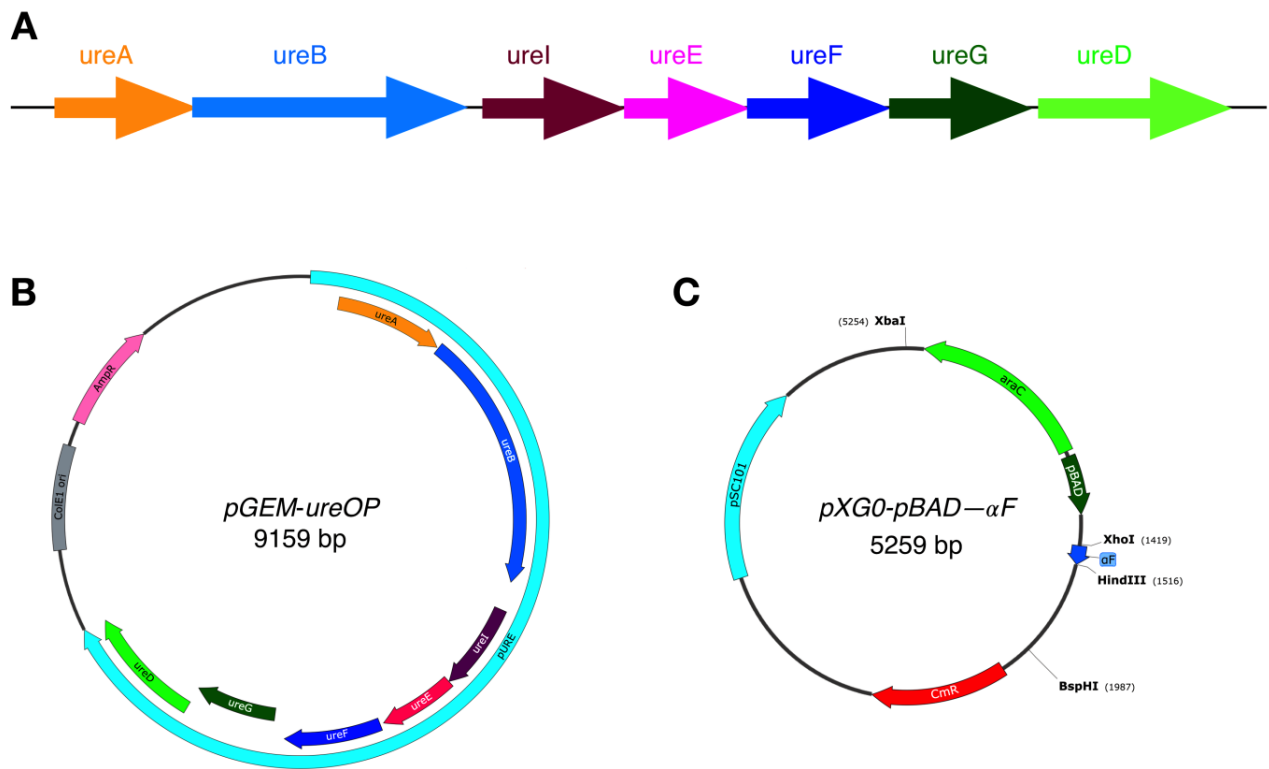


Figure 1. (A) *H. pylori* urease operon, cloned in a *pGEM-T-Easy* vector to yield *pGEM-ureOP* (B). The complementing plasmid, expressing αF under the expression control of arabinose promoter, is represented in (C).

To evaluate the urease activity in the cytoplasm of growing bacteria, the same genetic construct was used to transform Top10 *E. coli* cells. The recombinant bacteria maintained urease expression and activity, driven by the vector-encoded *lac* promoter upstream of the

1
2
3
169 *ure* operon. In addition, the *recA*- genotype of this strain ensured higher stability of the genetic
5
6
170 constructs, preventing unwanted recombination, especially when two plasmids harboring
8
171 similar sequences were co-transformed, a condition required for the experiments described
10
11
172 below.

13
173 The pH increase of the bacterial environment catalyzed by urease was used as a detection
15
174 system to evaluate the ureolytic capacity of the engineered *E. coli* strain, modifying a
17
18
175 previously reported protocol [21]. Indeed, the faster the urea hydrolysis, the more rapid and
20
21
176 distinct the increase of pH of the medium, resulting in a turning of a pH indicator, measured
22
23
177 as a change of absorbance whose slope is directly proportional to reaction rate. To find the
24
25
178 optimal assay conditions, the experiment was performed with different substrate and Ni(II)
27
28
179 concentrations (50 to 500 mM urea, Figure 2A; 0 to 750 μ M Ni(II), Figure 3), added to the
30
180 medium when cells reached the exponential growth. The dependence of the initial rate of
32
33
181 reaction on urea concentration (Figure 2B) decreases at substrate concentrations of 300 mM
34
35
182 urea, which is close to the maximal velocity of reaction (v_{max}) reached at 500 mM urea. These
37
38
183 data cannot be fit using a Michaelis-Menten treatment, possibly because other events, such
39
40
184 as urea penetration through the plasma membrane, influence the kinetics of the substrate
42
43
185 availability, and consequently affect the overall enzymatic reaction kinetics. It is interesting to
44
45
186 note that the K_M measured for urea hydrolysis by *H. pylori* urease is 0.17 mM or 0.79 mM [22]
46
47
187 *in vitro*, suggesting that only a minor fraction of urea is able to reach the cytoplasmatic
49
50
188 environment. Alternatively, this can be due to differences in the reaction conditions, such as
51
52
189 different pH, ionic strength, presence of competing molecules in the bacterial media, used
54
55
190 herein with respect to previous experiments carried out *in vitro* with purified urease.
56
57
58
59
60
61
62
63
64
65

1
2
3
191
5
6
7
8
9
10
11
12
13
14
15
16
17
18
19
20
21
22
23
24
25
26
27
192
29
193
194
195
196
197
198
199
200
37
38
39
201
41
202
43
44
203
45
46
204
48
49
205
50
51
52
53
54
55
56
57
58
59
60
61
62
63
64
65

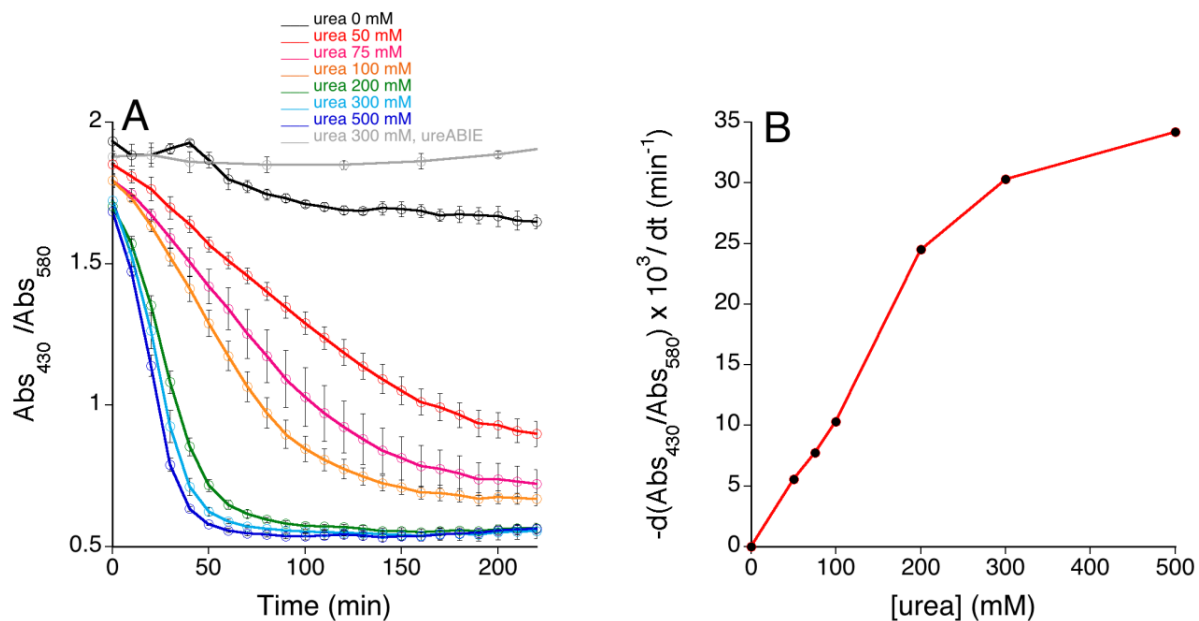


Figure 2. (A) Urease activity, measured as the ratio of absorbance at 430 nm and at 580 nm for the cresol red indicator, added to the *E. coli* culture harboring the *pGEM-ureOP* plasmid. The measures were performed in a 96-wells multiplate, after the addition of 250 μ M Ni(II) and different concentrations of urea, as indicated. The urease activity of an inactive strain, *ureABIE*, transformed with a defective urease operon lacking most urease accessory genes, is also shown for comparison. Every measure was performed in triplicate and the error bars represent the standard deviations of the average values. **(B)** Initial velocity of urea hydrolysis at different urea concentrations, measured as the slope of the first four points of the curves shown in (A).

The dependence of urease activity on Ni(II) concentration was tested both with substrate concentrations corresponding to a rate lower than half of v_{max} (75 mM, Figure 3A) and close to v_{max} (300 mM, Figure 3B). Under both conditions, no significant variation of hydrolysis rates was observed between 250 μ M and 750 μ M Ni(II), and therefore 250 μ M was the metal concentration added in all subsequent assays.

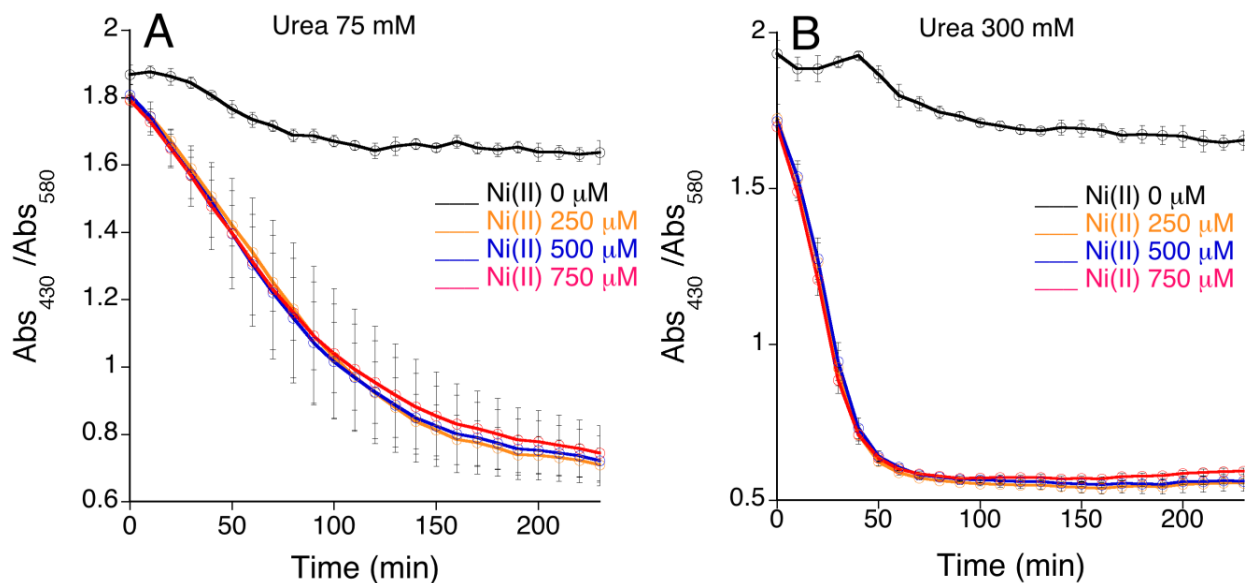


Figure 3. Urease activity, measured as the ratio of absorbance at 430 nm and at 580 nm for the cresol red indicator, added to the *E. coli* culture harboring the *pGEM-ureOP* plasmid. The measures were performed in a 96-wells multiplate, after the addition of different Ni(II) concentrations, as indicated, and of either 75 mM (A) or 300 mM (B) urea. Every measure was performed in triplicate and the error bars represent the standard deviations of the average values.

3.2. In-cell urease inhibition

To test the ability of known urease inhibitors to exert their action on the over-expressed enzyme in growing bacteria, these compounds were added at variable concentrations to the growth medium of *E. coli*, and the urease activity was measured as previously described. All inhibition assays were conducted at substrate concentration corresponding both to v_{max} (300 mM urea) and to a rate lower than half of v_{max} (75 mM urea) to evaluate the competitive nature of urease inhibition. Cultures that did not include the pH indicator were run in parallel to monitor the bacterial growth following the optical density at 600 nm, in order to exclude the toxicity of the tested molecules. In addition, equal dilutions of *E. coli* cultures, containing the highest inhibitor concentrations used, were plated at the end of each experiment and the number of colony forming units was compared with the ones generated in the absence of urease inhibitors. No significant variation in cell viability was observed for cells grown in the

1
2
3
225 presence of the selected compounds.
5

226 3.2.1. Fluoride and borate

8
227 Fluoride has been reported to exert a mixed inhibition with a predominance of an
10
11
228 uncompetitive mechanism[23]. While the uncompetitive inhibition constant remains
12
13
229 substantially stable in the pH range from 6.5 ($K_{iuc(F^-)} = 0.28$ mM) and 8 ($K_{iuc(F^-)} = 0.43$ mM) for
15
230 *Sporosarcina pasteurii* urease, the contribution of competitive inhibition is significant at pH 6.5
17
18
231 ($K_{ic(F^-)} = 0.79$ mM) and becomes negligible at pH 8[23]. The double mode of inhibition is
20
21
232 related to two fluoride ions bound to the enzyme active site: the first one, responsible for the
22
23
233 competitive inhibition, substitutes the substrate urea binding one of the two Ni(II) ions in the
24
25
234 active site, while the second one, involved in the uncompetitive inhibition, binds in place of the
27
28
235 nucleophilic hydroxide [23].

30
236 Differently, boric acid shows competitive inhibition in the form $B(OH)_3$, binding as a substrate
32
33
237 analogue to the enzyme active site and leaving in place the nucleophilic hydroxide[24].
34
35
238 Inhibition constants $K_{i(B(OH)_3)} = 0.099$ mM and 0.34 mM were reported for bacteria such as
37
239 *Proteus mirabilis* and *Klebsiella aerogenes* respectively[25].
39

40
240 Consistently with the inhibition constants measured *in vitro*, in-cell assays were conducted
42
241 with fluoride and borate concentrations between 0.5 mM and 5 mM, at 75 mM and 300 mM
44
45
242 urea concentrations (Figure 4). For both fluoride (Figure 4A) and borate (Figure 4B), the
46
47
243 inhibition effect resulted negligible, suggesting that these compounds are not able to
49
50
244 efficiently cross the plasma membrane of the Gram-negative *E. coli*. This observation proves
51
52
245 that the observed urease activity is ascribed to the cytoplasmatic urease, while the amount of
54
55
246 active enzyme in the extracellular medium is negligible.
56

1
2
3
247
5
6
7
8
9
10
11
12
13
14
15
16
17
18
19
20
21
22
23
24
25
26
248
27
28
29
250
251
252
253
254
255
256
257
258
259
260
261
262
263
264
265
266
267
268
269
270
271
272
273
274
275
276
277
278
279
280
281
282
283
284
285
286
287
288
289
290
291
292
293
294
295
296
297
298
299
300

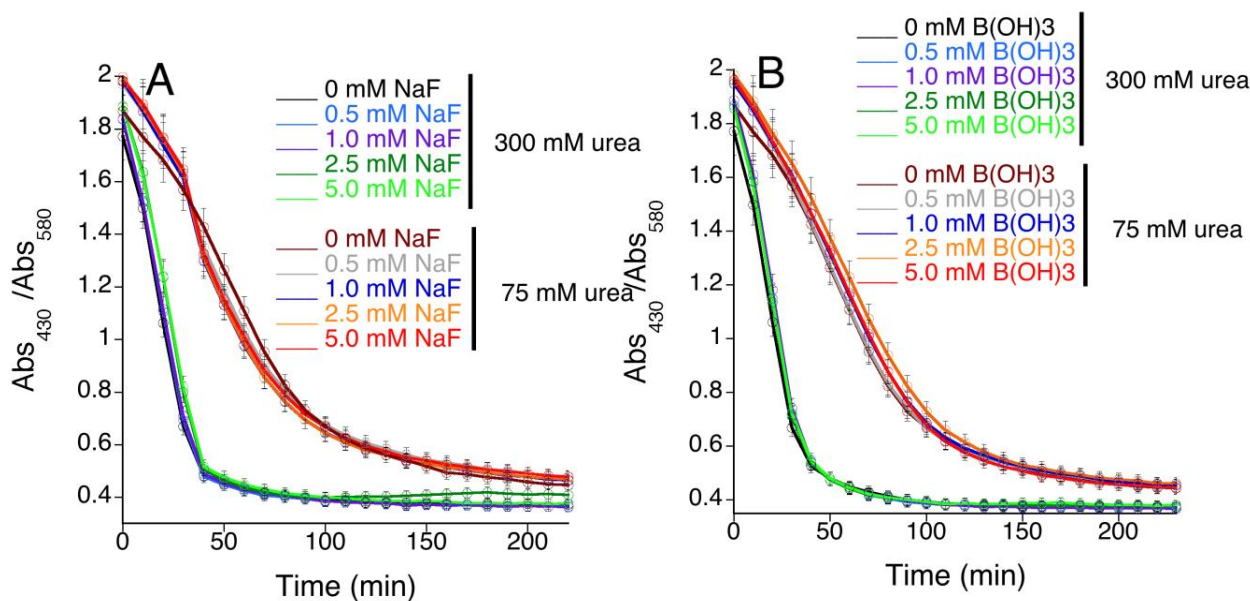


Figure 4. Urease activity, measured as the ratio of absorbance at 430 nm and at 580 nm for the cresol red indicator, added to the *E. coli* culture harboring the *pGEM-ureOP* plasmid, in the presence of increasing concentrations of fluoride (A) or boric acid (B) urease inhibitors. The measures were performed in a 96-wells multiplate, after the addition of 250 μ M Ni(II) and of 75 mM and 300 mM urea. Every measure was performed in triplicate. The error bars represent the standard deviations of the average values.

3.2.2. AHA and NBPT

Aceto-hydroxamic acid (AHA) and N-(n-butyl)-thiophosphoric triamide (NBPT) are well-known competitive, slow binding, urease inhibitors. AHA binds the urease active site with the hydroxamate oxygen atom bridging the two Ni(II) ions, while the carbonyl oxygen chelates one Ni(II) ion.[26–28] This compound shows a bactericidal effect on *H. pylori*,[29] and is the only urease inhibitor used in therapy to treat urinary tract infections[30], despite its severe side effects such as teratogenicity and toxicity[31]. The *in vitro* inhibition constant for *H. pylori* urease is $K_{i(AHA)} = 2 \mu$ M [32]. In this in-cell assay, high concentrations (1 mM) of AHA added to the medium show a partial reduction of urease activity only at lower urea concentrations, supporting the competitive nature of AHA inhibition observed *in vitro* (Figure 5). An $IC_{50} = 1.1$ mM can be derived by the data at 75 mM urea, similar to the IC_{50} measured for *H. pylori* J99

1
2
3
266
5
267
8
268
10
269
12
13
14
15
16
17
18
19
20
21
22
23
24
25
26
27
28
29
30
31
32
270
34
35
271
272
273
274
275
40
276
42
277
44
45
278
46
47
279
49
280
51
52
281
54
282
56
57
283
58
59
284
61
62
63
64
65

strain, reported between 1.35 mM and 1.66 mM [33]. The high AHA concentrations needed to obtain urease inhibition suggest the partial absorption of AHA by the *E. coli* membrane, and provides a rationale for the large doses (~ 1000 mg/day for adults) required for its administration *in vivo* [34].

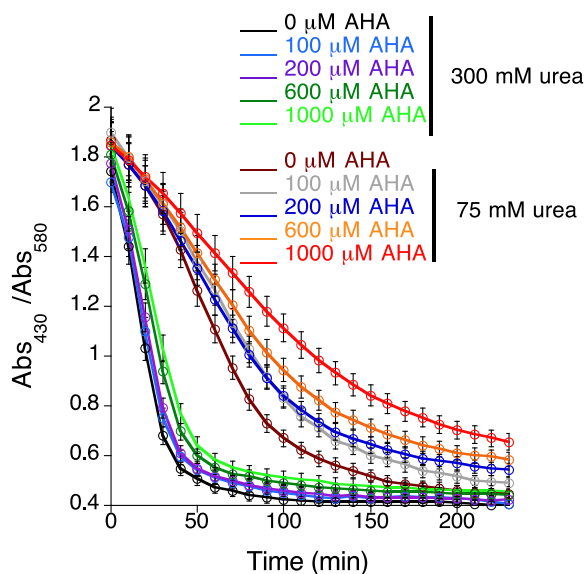


Figure 5. Urease activity, measured as the ratio of absorbance at 430 nm and at 580 nm for the cresol red indicator, added to the *E. coli* culture harboring the *pGEM-ureOP* plasmid, in the presence of increasing concentrations of AHA inhibitor, as indicated. The measures were performed in a 96-wells multiplate, after the addition of 250 μM Ni(II) and of 75 mM and 300 mM urea. Every measure was performed in triplicate. The error bars represent the standard deviations of the average values.

On the other hand, NBPT interacts with urease after an initial hydrolytic event that forms the mono-deaminated form (NBPD), which is further hydrolyzed in the presence of urease forming monoamine thiophosphate (MATP); the latter thus coordinates the Ni(II) ions in the active site of the enzyme [35]. The NBPT competitive inhibition constant is $K_{ic(NBPT)}$ 6.4 μM for *S. pasteurii* urease and 0.94 μM for jack bean urease [35]. In bacterial cultures, NBPT was active both at lower (Figure 6A) and at higher (Figure 6B) urea concentrations, showing an IC_{50} of 23 μM and 31 μM respectively. The lower value for IC_{50} obtained at low urea concentrations is consistent with its competitive inhibition mechanism.

1
2
3
285
5
6
7
8
9
10
11
12
13
14
15
16
17
18
19
20
21
22
23
24
25
26
286
28
287
288
289
290
291
292
35
36
293
38
294
40
41
295
43
296
45
46
297
48
298
50
299
52
300
55
301
56
302
58
303
60
61
62
63
64
65

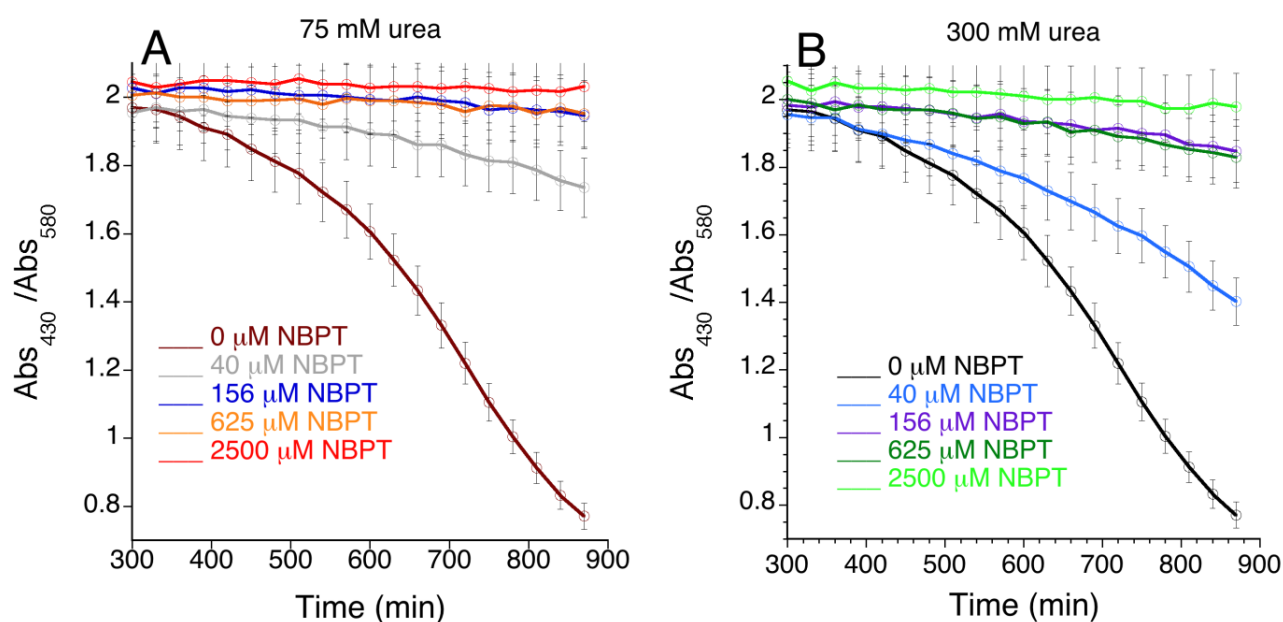
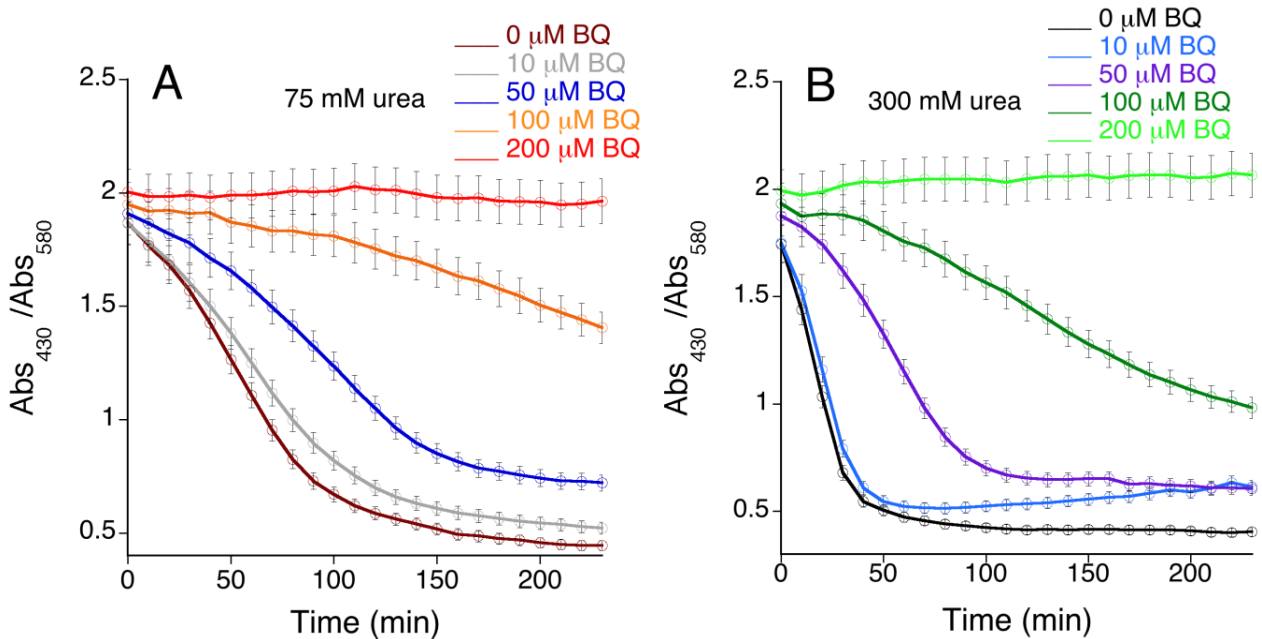


Figure 6. Urease activity, measured as the ratio of absorbance at 430 nm and at 580 nm for the cresol red indicator, added to the *E. coli* culture harboring the *pGEM-ureOP* plasmid, in the presence of increasing concentrations of NBPT inhibitor. The measures were performed in a 96-wells multiplate, after the addition of 250 μM Ni(II) and of 75 mM (A) and 300 mM (B) urea. Every measure was performed in triplicate. The error bars represent the standard deviations of the average values.

3.2.3. 1,4-benzoquinone

A distinctive inhibition mechanism is observed in the case of quinones. These compounds easily react with thiols to give the thiol-substituted benzene-1,4-diol. In particular, the crystal structure of urease inhibited by 1,4-benzoquinone (BQ) indicates that this compounds targets the conserved Cys residue present in the flap regulating the access to the active site pocket[36]. Covalent modifications of this residue lead to enzyme inactivation. This is consistent with the observed process of uncompetitive enzyme inhibition, with a kinetic constant $k = 1.24 \pm 0.06 \times 10^3 \text{ M}^{-1} \text{ s}^{-1}$ [36]. The minimum concentration of BQ required to observe this effect *in vitro* is 18 μM [36]. In-cell, BQ shows an inhibitory effect both at lower (Figure 7A) and higher (Figure 7B) substrate concentrations, with a calculated IC_{50} of 55 μM in both conditions. This observation confirms, *in vivo*, the uncompetitive nature of the

1
2
3
304 inhibition reported *in vitro*. The concentration range of BQ effect is comparable in cell and *in*
5
6
305 *vitro*, suggesting that this compound is able to efficiently move through the Gram-negative
8
306 plasma membrane.



310 **Figure 7.** Urease activity, measured as the ratio of absorbance at 430 nm and at 580 nm for the cresol red
311 indicator, added to the *E. coli* culture harboring the *pGEM-ureOP* plasmid, in the presence of increasing
312 concentrations of benzoquinone inhibitor. The measures were performed in a 96-wells multiplate, after the
313 addition of 250 μM Ni(II) and of either 75 mM (A) or 300 mM (B) urea. Every measure was performed in
314 triplicate. The error bars represent the standard deviations of the average values.

316 3.3. In-cell inhibition of urease maturation

317 A possible alternative route to inhibit urease activity is to prevent the construction of the active
318 site that requires Ni(II) ions insertion, targeting the protein-protein interactions (PPIs) between
319 the chaperones that carry out urease maturation. To identify the interaction “hot spots”, that is
320 the protein segments that contribute most significantly to the binding interface indicative for
321 the most promising “druggable” interfaces, the Peptiderive protocol [37]
322 (<http://rosie.rosettacommons.org/peptiderive>) was applied, starting from the crystal structure
323 of the UreF₂-UreD₂ heterodimer [38] (Figure 8A). When UreD was assigned as the receptor

1
2
3
4
5
6
7
8
9
10
11
12
13
14
15
16
17
18
19
20
21
22
23
24
25
26
27
28
29
30
31
32
33
34
35
36
37
38
39
40
41
42
43
44
45
46
47
48
49
50
51
52
53
54
55
56
57
58
59
60
61
62
63
64
65

for the peptide, and a query for a sequence of 10 and 20 residues was submitted for the inhibitor peptide, the protocol detected a hot spot region at the C-termini of the UreF sequence (D²²⁶ESHLCTAS**SVQNDIKAMQHE**²⁴⁵ for the 20 residue segment, the 10 residue segment is represented in bold), including an α -helical motif (underlined) that, in the crystal structure, makes extended contacts with UreD (Figure 8A) [38]. This sequence is located in a protein region that is degraded from Ser²³⁴ due to disorder when UreF is expressed in the absence of its partner[39], therefore suggesting that the PPI is stable enough to protect this part from proteolytic cleavage. This observation also implies that this interaction involves a disorder-to-order transition. To confirm the role of this sequence in the PPI, we mutated the *ureF* gene found in the *pGEM-ureOP* genetic construct, introducing a stop codon at position 233 to delete the region (here called α F) containing the C-terminal 21 residues of the protein. The recombinant strain produced a urease-inactive culture, proving that this protein segment is essential for the formation of an active UreF₂-UreD₂ complex and consequent urease activation in the bacteria (Figure 8B, light blue curve). A similar urease-negative phenotype was observed with *E. coli* transformed with *pGEM-ureABIE* vector, which lacks the accessory genes *ureF*, *ureD* and *ureG* genes (Figure 8B, orange curve).

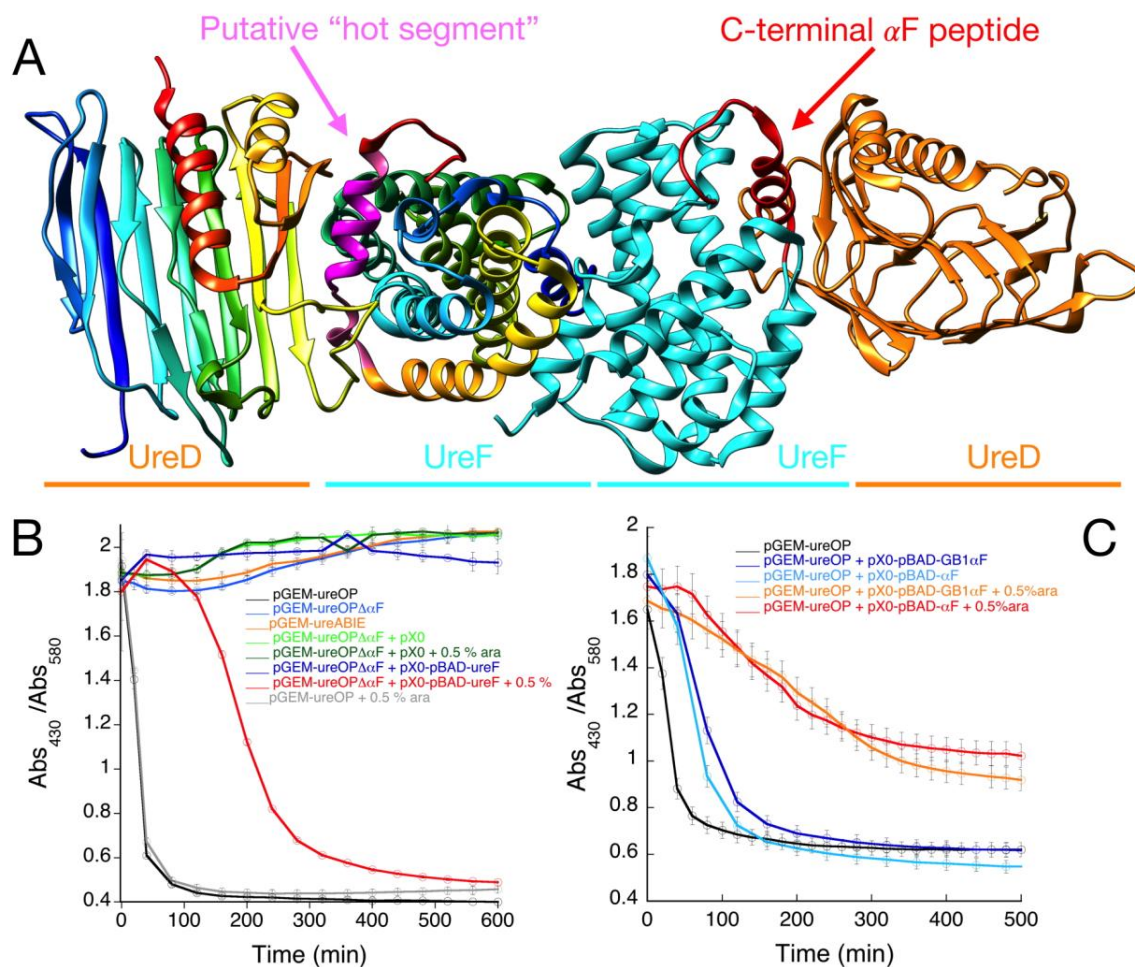


Figure 8. (A) Crystal structure of the UreD₂-UreF₂ complex (PDB code: 3SF5). For each protein, a chain is represented coloring successive residues from blue (N-terminus) to red (C-terminus). The second chain is colored in cyan (UreF) or in orange (UreD). The C-terminal segment of UreF (αF, in magenta) is sensitive to proteolysis and is preserved only upon the PPI. The "hot segments" found by Peptiderive are depicted in pink (20-residue segment) and in magenta (10-residue segment). (B) Urease activity, measured as the ratio of absorbance at 430 nm and at 580 nm for the cresol red indicator, added to the *E. coli* culture harboring *pGEM-ureOP*, either in the wild type or the mutated versions, both alone or complemented with empty *pXG0* or *pXG0-pBAD-ureF* plasmids. When indicated, 0.5 % arabinose inducer was added to the bacterial culture. The measures were performed in a 96-wells multiplate, after the addition of 250 μM Ni(II) and 300 mM urea. Every measure was performed in triplicate and the error bars represent the standard deviations of the average values. (C) Urease activity, measured as the ratio of absorbance at 430 nm and at 580 nm for the cresol red indicator added to the *E. coli* culture harboring wild-type *pGEM-ureOP* alone or co-transformed with *pXG0-pBAD-GB1-αF* or *pXG0-pBAD-αF* plasmids. When indicated, 0.5 % arabinose inducer was added to the bacterial culture. The measures were performed in a 96-wells multiplate, after the addition of 250 μM Ni(II) and 300 mM urea. Every measure was performed in triplicate and the error bars represent the standard deviations of the average values.

1
2
3
361 A second plasmid carrying a copy of the wild-type *ureF* gene under the control of the
5
362 arabinose promoter (*pBAD*) and with an origin of replication compatible with the *pGEM-ureOP*
6
363 plasmid was produced (Figure 1C and S11) and this construct, named *pXG0-pBAD-ureF*, was
8
364 able to complement the mutation in a co-transformed strain only in the presence of arabinose
10
365 inducer (Figure 8B, red curve). No complementation was observed in the absence of
11
366 arabinose (Figure 8B, blue curve) or when the co-transformed plasmid did not contain the
12
367 *ureF* gene (Figure 8B, light green and green curves).
13
14
15
16
17
18
19
20
21
22
23
24
25
26
27
28
29
30
31
32
33
34
35
36
37
38
39
40
41
42
43
44
45
46
47
48
49
50
51
52
53
54
55
56
57
58
59
60
61
62
63
64
65

This two-plasmid system was then used to prove the ability of the α F peptide to inhibit, after induction, in-cell urease activity. Arabinose-induced co-expression of the peptide (sequence MGSGSGSSVQNDIKAMQHESLYSRLYMS, UreF sequence underlined), alone (Figure 8C, red line) or fused to the C-terminus of the small globular protein GB1 [40] (Figure 8C, orange line), sensibly decreased the in-cell urease activity as compared to bacteria expressing the wild-type operon (Figure 8C, black line) or to the co-transformed bacteria in the absence of arabinose induction (Figure 8C, blue and light blue lines). Therefore, the identified sequence represents a leading interfering peptide to inhibit the urease activating PPIs.

1
2
3
377
5
6
378
379
9
380
11
12
381
13
14
382
16
17
383
18
19
384
21
22
385
23
24
386
26
27
387
28
29
388
31
389
33
34
390
35
36
391
38
39
392
40
41
393
43
44
394
45
46
395
48
49
396
50
51
397
52
53
398
55
56
399
57
58
400
60
61
401
62
63
64
65

4. Discussion

Urease is an essential virulence factor for *H. pylori* colonization of the human stomach and represents an attractive target for the development of antimicrobial strategies to counteract the increasingly emergent problem of antimicrobial resistance of this bacterium. Urease inactivation might be accomplished i) by designing specific enzyme inhibitors that selectively bind the active site of urease, preventing substrate binding and catalysis, or ii) by interrupting the protein-protein interaction (PPI) network that leads to Ni(II) delivery into the active site, precluding enzyme maturation. The first approach has been thoroughly pursued by searching for urease inhibitors that directly bind the Ni(II) ions in the active site or interfere with the catalytic cycle. Nevertheless, despite the large number of known urease inhibitors, this potential therapeutic route showed very limited success to date, with only few compounds evaluated in therapeutic studies presenting efficiency and safety concerns for their use *in vivo* [41]. Indeed, many drugs are not effective in therapy, or require very high dosage because of their low stability or limited bioavailability, not being able to efficiently diffuse inside the Gram-negative plasma membrane of the bacterium to reach their target in the cytoplasm. In this work, we addressed this problem by developing and optimizing a novel high-throughput screening system that allows to determine the capability of urease inhibitors directly in a physiological cell environment. In the past, the activity of urease was measured in the soluble fraction of the cellular extract after cellular lysis[18], and in batch measurements on whole *E. coli* cells resuspended in phosphate-buffered saline (PBS) buffer, incubated with urea and tested for urease activity at different time points [42]. Here, we took advantage of an ureolytic *E. coli* model system, obtained by transforming a commercial bacterial strain with a previously engineered plasmid expressing the urease operon (Figure 1)[18]. Bacterial cultures were then

1
2
3
4
5
6
7
8
9
10
11
12
13
14
15
16
17
18
19
20
21
22
23
24
25
26
27
28
29
30
31
32
33
34
35
36
37
38
39
40
41
42
43
44
45
46
47
48
49
50
51
52
53
54
55
56
57
58
59
60
61
62
63
64
65

grown in a 96-well plate and the in-cell urease activity was measured over time during cell growth at diverse concentrations of urea and Ni(II), applying a well-established pH-dependent colorimetric assay (Figure 2 and 3). Subsequently, the optimized assay conditions were used to test different types and concentrations of known urease inhibitors with a high-throughput (HT) approach. Interestingly, we found that well-known urease inhibitors such as boric acid and fluoride (Figure 4) were unable to exert their inhibition effect on the cytoplasmatic urease, probably because of their incapability to penetrate into the bacteria. A known competitive inhibitor such acetohydroxamic acid (AHA), which has some known applications in therapy, demonstrated a moderate decrease of in-cell enzymatic activity only at high concentrations and at lower substrate concentrations (Figure 5), indicating the preservation of the competitive inhibition mechanism, as well as revealing its limited bioavailability. On the other hand, the efficacy of the competitive and slow-binding inhibitor N-(n-butyl)-thiophosphoric triamide (NBPT, Figure 6) and of the uncompetitive inhibitor 1,4-benzoquinone (BQ, Figure 7) proved to be conserved in cell at the concentrations effective *in vitro*. Notably, this means that BQ and NBPT (and/or its hydrolyzed derivative NBPD) are able to penetrate the cytoplasmic membrane and carry out urease inhibition within the cell. This is consistent with recent reports of NBPT being able to decrease the growth of ureolytic bacteria such as *S. pasteurii* [43] as well as with older evidence for NBPT toxicity for plants [44–50]. Therefore, the use of the well-characterized Gram-negative *E. coli* as a model for drug administration to the pathogenic bacterium *H. pylori*, whose slow growth and absence of standard genetic tools hampers the implementation of HT assays, proved to be a robust and cost-effective prototype to directly evaluate membrane permeability and urease inhibition of a large number of compounds.

An alternative route to inhibit urease is to prevent the Ni(II) ions insertion into the active site, blocking the PPIs between the urease metallo-chaperones. This is a strategy yet unexplored

1
2
3
4
5
6
7
8
9
10
11
12
13
14
15
16
17
18
19
20
21
22
23
24
25
26
27
28
29
30
31
32
33
34
35
36
37
38
39
40
41
42
43
44
45
46
47
48
49
50
51
52
53
54
55
56
57
58
59
60
61
62
63
64
65

426 that might bring innovative solutions. Within this type of approach, a bismuth-based drug, a
427 known treatment against *H. pylori* that impacts on the activity of urease, was recently found to
428 impair the function of the accessory protein UreG, and thus the urease maturation, resulting in
429 the attenuated virulence of the pathogen [51].

430 Although the identification of selective, potent and effective inhibitors for PPIs is more difficult
431 than for traditional targets, largely because of the extended nature of the PPI interfaces,
432 remarkable progresses have been made in discovery, characterization and development of
433 small molecules (SMs) as PPI inhibitors in the recent years[52]. These successes are due to
434 the finding of the importance for the interaction of a limited number of “hot spot” residues at
435 the protein interfaces, often included in a short peptide, estimated to contribute most
436 significantly to the binding energy between the protein partners[53]. The ability to localize
437 these “hot segments” in protein-protein interfaces has been crucial for providing an optimal
438 lead for drug design, because these peptides can compete with the proteins from which they
439 were derived, hindering the binding to the cognate interactors.

440 Based on the structural information available and using the Peptiderive protocol [37], we
441 could identify, at the dimer interface of the UreF₂-UreD₂ complex, a peptide from the C-termini
442 of UreF largely involved in the interaction with UreD, thus possibly interfering, if expressed
443 alone, with this PPI. This region is likely affected by intrinsic disorder in the isolated protein,
444 as revealed by its proteolytic degradation when UreF is expressed in the absence of its
445 partner, while it undergoes folding into an α -helical structure upon interaction with UreD.
446 Typically, PPIs that require folding upon binding are more easily blocked by SMs, and thus
447 this interface represents an ideal target for drug discovery[54,55]. In addition, this part of the
448 complex contains a Ni(II) binding site, likely being part of the route for Ni(II) delivery into

1
2
3
449 urease [18,56,57]. Disrupting such interaction interface therefore provides a promising
5
6
450 strategy to prevent Ni(II) delivery and consequent urease maturation.
7
8

451 Using the genetic tools of the *E. coli* model, we developed a two-plasmids system to prove
10
11
452 the essentiality of this segment for the formation of a productive PPI, by C-terminal truncation
12
13
453 of the *ureF* gene on the urease operon and subsequent complementation with the wild type
15
16
454 gene (Figure 8). These results showed that this interface represents a promising region to be
17
18
455 targeted with a SM that mimics the UreF C-terminal peptide sequence.
19
20
21

22
456 Oligopeptides are often used for interfering with protein interaction sites, as their modular
23
24
457 nature, the low toxicity, and the possibility to screen a large number of molecules through
26
27
458 combinatorial approaches, render these chemical species a favorable solution. However,
28
29
459 screening and optimizing peptide sequences has been challenging due to the difficulty of
31
32
460 these molecules to penetrate the cellular membrane. To explore the ability of the identified
33
34
461 peptide to inhibit urease activity in the intracellular environment, we applied the newly
35
36
462 developed two-plasmid system to co-express, together with the wild type urease enzyme, the
38
39
463 candidate sequence. We found that induction of peptide expression significantly reduced
40
41
464 urease activity in cell – while no inhibition was observed in the absence of the arabinose
43
44
465 inducer - therefore proving that the identified sequence represents a promising lead peptide
45
46
466 structure (Figure 8).
48
49

50
467 The two-plasmid system described here has the potential to significantly facilitate the
51
52
468 screening process of interfering peptides, as the candidates can be generated intracellularly
54
55
469 and, starting from the C-terminal segment of UreF, undergo mutagenesis and in-cell testing
56
57
470 for the phenotype-specific inhibition using the in-cell assay described above. This would avoid
58
59
471 the need of expensive peptide synthesis, as well as of protein and peptide purification. This
61
62
63
64
65

1
2
3
472 strategy, based on directed evolution to dissect PPIs, is emerging as a way to generate
5
6
473 variants with increasing affinity for the protein interfaces [58]. In addition, the possibility of
8
474 studying the biological role of PPIs in a native cellular environment is fundamental to avoid
10
11
475 artifacts and drive data interpretations. The identified interfering sequence can be the basis
12
13
476 for future work of drug design of peptidomimetics and SMs with higher pharmacological
15
16
477 potential.

17
18
19
478 In conclusion, this work describes a robust and reliable method to evaluate, directly in the cell,
21
22
479 the drug potential of known *H. pylori* urease inhibitors with diverse action modes, such as
23
24
480 competitive, uncompetitive or slow-binding, as well as the role of interfering peptides in
26
27
481 interrupting the PPI network leading to urease maturation. The developed system renders
28
29
482 thus feasible the concomitant screening of a large number of drug candidates that interfere
31
32
483 with the enzyme activity both at the level of the enzyme catalysis and maturation. Among the
33
34
484 twelve most important bacteria listed in 2017 by WHO as a global threat because of the
35
36
485 emerging development of antimicrobial resistance (<https://goo.gl/vLRURp>) [7], ten produce
38
39
486 urease, the activity of which is demonstrated as a pathogenic factor for some of them, beside
40
41
487 *H. pylori*: for example, *Pseudomonas aeruginosa* and *Staphylococcus aureus* urease activity
43
44
488 determines biofilm formation [59,60], for *P. mirabilis* [61], *Staphylococcus saprophyticus* [62]
45
46
489 and *Ureaplasma urealyticum* [63] urease activity plays a central role for infection and urea
48
490 stones formation in the urinary tract. Inhibition of this enzyme has therefore the potential of
50
51
491 being a global antibacterial strategy for a large number of infections. This work paves the way
52
53
492 for the development and evolution of new drug candidates that can be applied, in the future,
55
56
493 also to other bacterial targets.

58
494
60
61
62
63
64
65

1
2
3
495
5
6
496
8
497
10
11
498
12
13
499
15
500
17
18
501
20
502
22
23
503
25
504
27
28
29
30
31
32
33
34
35
36
37
38
39
40
41
42
43
44
45
46
47
48
49
50
51
52
53
54
55
56
57
58
59
60
61
62
63
64
65

5. Acknowledgements

This work was supported by the Department of Pharmacy and Biotechnology of the University of Bologna through funds for fundamental research (to BZ, AD and SC) and grant FARB Project RFBO120249 of the Department of Pharmacy and Biotechnology. The authors also thank Dr Luca Mazzei for useful discussions on the experimental set up of the in cell assays.

1
2
3
505
5
6
506
8
507
10
508
12
509
15
510
17
511
20
512
22
513
24
514
27
515
29
516
32
517
34
518
37
519
39
520
42
521
44
522
46
523
49
524
51
525
54
526
56
527
58
528
61
62
63
64
65

6. References

- [1] T.L. Testerman, J. Morris, Beyond the stomach: an updated view of *Helicobacter pylori* pathogenesis, diagnosis, and treatment., *World J. Gastroenterol.* 20 (2014) 12781–808. doi:10.3748/wjg.v20.i36.12781.
- [2] IARC, Schistosomes, liver flukes and *Helicobacter pylori*., 1994. doi:PMID 7715068.
- [3] IARC, *Helicobacter pylori*, in: IARC Monogr. – 100B, Lyon - France, 2012: pp. 385–435. <http://monographs.iarc.fr/ENG/Monographs/vol100B/mono100B-15.pdf> (accessed April 28, 2018).
- [4] IARC, *Helicobacter pylori* Eradication as a Strategy for Preventing Gastric Cancer, (2014). <http://www.iarc.fr/en/publications/pdfs-online/wrk/wrk8/index.php> (accessed April 4, 2018).
- [5] A. Stathis, F. Bertoni, E. Zucca, Treatment of gastric marginal zone lymphoma of MALT type, *Expert Opin. Pharmacother.* 11 (2010) 2141–2152. doi:10.1517/14656566.2010.497141.
- [6] N.J. Talley, K.M. Fock, P. Moayyedi, Gastric Cancer Consensus conference recommends *Helicobacter pylori* screening and treatment in asymptomatic persons from high-risk populations to prevent gastric cancer., in: *Am. J. Gastroenterol.*, 2008: pp. 510–514. doi:10.1111/j.1572-0241.2008.01819.x.
- [7] W.H.O. WHO, Global priority list of antibiotic-resistant bacteria to guide research, discovery, and development of new antibiotics, n.d.
- [8] B. Zambelli, F. Musiani, S. Benini, S. Ciurli, Chemistry of Ni²⁺ in urease: Sensing, trafficking, and catalysis, *Acc. Chem. Res.* 44 (2011) 520–530. doi:10.1021/ar200041k.
- [9] B. Zambelli, S. Ciurli, Nickel and human health, *Met. Ions Life Sci.* 13 (2013) 321–357.

- 1
2
3
529 doi:10.1007/978-94-007-7500-8-10.
5
6
530 [10] K.A. Eaton, C.L. Brooks, D.R. Morgan, S. Krakowka, Essential Role of Urease in
8
531 Pathogenesis of Gastritis Induced by *Helicobacter pylori* in Gnotobiotic Piglets, Infect.
10
532 Immun. 59 (1991) 2470–2475.
11
12
13
533 [11] K.A. Eaton, S. Krakowka, Effect of gastric pH on urease-dependent colonization of
15
534 gnotobiotic piglets by *Helicobacter pylori*, Infect. Immun. 62 (1994) 3604–3607.
16
17
18
535 [12] M. Campanale, E. Nucera, V. Ojetti, V. Cesario, T.A. Di Rienzo, G. D’Angelo, S.
20
536 Pecere, F. Barbaro, G. Gigante, T. De Pasquale, A. Rizzi, G. Cammarota, D. Schiavino,
22
537 F. Franceschi, A. Gasbarrini, Nickel free-diet enhances the *Helicobacter pylori*
23
538 eradication rate: A pilot study, Dig. Dis. Sci. 59 (2014) 1851–1855.
24
25
539 [http://eutils.ncbi.nlm.nih.gov/entrez/eutils/elink.fcgi?dbfrom=pubmed&](http://eutils.ncbi.nlm.nih.gov/entrez/eutils/elink.fcgi?dbfrom=pubmed&id=24595654)
27
540 [id=24595654](http://eutils.ncbi.nlm.nih.gov/entrez/eutils/elink.fcgi?dbfrom=pubmed&id=24595654)
28
541 [http://eutils.ncbi.nlm.nih.gov/entrez/eutils/elink.fcgi?dbfrom=pubmed&](http://eutils.ncbi.nlm.nih.gov/entrez/eutils/elink.fcgi?dbfrom=pubmed&id=24595654)
30
542 [id=24595654](http://eutils.ncbi.nlm.nih.gov/entrez/eutils/elink.fcgi?dbfrom=pubmed&id=24595654)
31
543 [http://eutils.ncbi.nlm.nih.gov/entrez/eutils/elink.fcgi?dbfrom=pubmed&](http://eutils.ncbi.nlm.nih.gov/entrez/eutils/elink.fcgi?dbfrom=pubmed&id=24595654)
32
544 [id=24595654](http://eutils.ncbi.nlm.nih.gov/entrez/eutils/elink.fcgi?dbfrom=pubmed&id=24595654)
33
545 [http://eutils.ncbi.nlm.nih.gov/entrez/eutils/elink.fcgi?dbfrom=pubmed&](http://eutils.ncbi.nlm.nih.gov/entrez/eutils/elink.fcgi?dbfrom=pubmed&id=24595654)
34
546 [id=24595654](http://eutils.ncbi.nlm.nih.gov/entrez/eutils/elink.fcgi?dbfrom=pubmed&id=24595654)
35
547 [http://eutils.ncbi.nlm.nih.gov/entrez/eutils/elink.fcgi?dbfrom=pubmed&](http://eutils.ncbi.nlm.nih.gov/entrez/eutils/elink.fcgi?dbfrom=pubmed&id=24595654)
36
548 [id=24595654](http://eutils.ncbi.nlm.nih.gov/entrez/eutils/elink.fcgi?dbfrom=pubmed&id=24595654)
37
549 [http://eutils.ncbi.nlm.nih.gov/entrez/eutils/elink.fcgi?dbfrom=pubmed&](http://eutils.ncbi.nlm.nih.gov/entrez/eutils/elink.fcgi?dbfrom=pubmed&id=24595654)
38
550 [id=24595654](http://eutils.ncbi.nlm.nih.gov/entrez/eutils/elink.fcgi?dbfrom=pubmed&id=24595654)
39
551 [http://eutils.ncbi.nlm.nih.gov/entrez/eutils/elink.fcgi?dbfrom=pubmed&](http://eutils.ncbi.nlm.nih.gov/entrez/eutils/elink.fcgi?dbfrom=pubmed&id=24595654)
40
552 [id=24595654](http://eutils.ncbi.nlm.nih.gov/entrez/eutils/elink.fcgi?dbfrom=pubmed&id=24595654)
41
553 [http://eutils.ncbi.nlm.nih.gov/entrez/eutils/elink.fcgi?dbfrom=pubmed&](http://eutils.ncbi.nlm.nih.gov/entrez/eutils/elink.fcgi?dbfrom=pubmed&id=24595654)
42
554 [id=24595654](http://eutils.ncbi.nlm.nih.gov/entrez/eutils/elink.fcgi?dbfrom=pubmed&id=24595654)
43
555 [http://eutils.ncbi.nlm.nih.gov/entrez/eutils/elink.fcgi?dbfrom=pubmed&](http://eutils.ncbi.nlm.nih.gov/entrez/eutils/elink.fcgi?dbfrom=pubmed&id=24595654)
44
556 [id=24595654](http://eutils.ncbi.nlm.nih.gov/entrez/eutils/elink.fcgi?dbfrom=pubmed&id=24595654)
45
557 [http://eutils.ncbi.nlm.nih.gov/entrez/eutils/elink.fcgi?dbfrom=pubmed&](http://eutils.ncbi.nlm.nih.gov/entrez/eutils/elink.fcgi?dbfrom=pubmed&id=24595654)
46
558 [id=24595654](http://eutils.ncbi.nlm.nih.gov/entrez/eutils/elink.fcgi?dbfrom=pubmed&id=24595654)
47
559 [http://eutils.ncbi.nlm.nih.gov/entrez/eutils/elink.fcgi?dbfrom=pubmed&](http://eutils.ncbi.nlm.nih.gov/entrez/eutils/elink.fcgi?dbfrom=pubmed&id=24595654)
48
560 [id=24595654](http://eutils.ncbi.nlm.nih.gov/entrez/eutils/elink.fcgi?dbfrom=pubmed&id=24595654)
49
561 [http://eutils.ncbi.nlm.nih.gov/entrez/eutils/elink.fcgi?dbfrom=pubmed&](http://eutils.ncbi.nlm.nih.gov/entrez/eutils/elink.fcgi?dbfrom=pubmed&id=24595654)
50
562 [id=24595654](http://eutils.ncbi.nlm.nih.gov/entrez/eutils/elink.fcgi?dbfrom=pubmed&id=24595654)
51
563 [http://eutils.ncbi.nlm.nih.gov/entrez/eutils/elink.fcgi?dbfrom=pubmed&](http://eutils.ncbi.nlm.nih.gov/entrez/eutils/elink.fcgi?dbfrom=pubmed&id=24595654)
52
564 [id=24595654](http://eutils.ncbi.nlm.nih.gov/entrez/eutils/elink.fcgi?dbfrom=pubmed&id=24595654)
53
565 [http://eutils.ncbi.nlm.nih.gov/entrez/eutils/elink.fcgi?dbfrom=pubmed&](http://eutils.ncbi.nlm.nih.gov/entrez/eutils/elink.fcgi?dbfrom=pubmed&id=24595654)
54
566 [id=24595654](http://eutils.ncbi.nlm.nih.gov/entrez/eutils/elink.fcgi?dbfrom=pubmed&id=24595654)
55
567 [http://eutils.ncbi.nlm.nih.gov/entrez/eutils/elink.fcgi?dbfrom=pubmed&](http://eutils.ncbi.nlm.nih.gov/entrez/eutils/elink.fcgi?dbfrom=pubmed&id=24595654)
56
568 [id=24595654](http://eutils.ncbi.nlm.nih.gov/entrez/eutils/elink.fcgi?dbfrom=pubmed&id=24595654)
57
569 [http://eutils.ncbi.nlm.nih.gov/entrez/eutils/elink.fcgi?dbfrom=pubmed&](http://eutils.ncbi.nlm.nih.gov/entrez/eutils/elink.fcgi?dbfrom=pubmed&id=24595654)
58
570 [id=24595654](http://eutils.ncbi.nlm.nih.gov/entrez/eutils/elink.fcgi?dbfrom=pubmed&id=24595654)
59
571 [http://eutils.ncbi.nlm.nih.gov/entrez/eutils/elink.fcgi?dbfrom=pubmed&](http://eutils.ncbi.nlm.nih.gov/entrez/eutils/elink.fcgi?dbfrom=pubmed&id=24595654)
60
572 [id=24595654](http://eutils.ncbi.nlm.nih.gov/entrez/eutils/elink.fcgi?dbfrom=pubmed&id=24595654)
61
573 [http://eutils.ncbi.nlm.nih.gov/entrez/eutils/elink.fcgi?dbfrom=pubmed&](http://eutils.ncbi.nlm.nih.gov/entrez/eutils/elink.fcgi?dbfrom=pubmed&id=24595654)
62
574 [id=24595654](http://eutils.ncbi.nlm.nih.gov/entrez/eutils/elink.fcgi?dbfrom=pubmed&id=24595654)
63
575 [http://eutils.ncbi.nlm.nih.gov/entrez/eutils/elink.fcgi?dbfrom=pubmed&](http://eutils.ncbi.nlm.nih.gov/entrez/eutils/elink.fcgi?dbfrom=pubmed&id=24595654)
64
576 [id=24595654](http://eutils.ncbi.nlm.nih.gov/entrez/eutils/elink.fcgi?dbfrom=pubmed&id=24595654)
65
- [10] K.A. Eaton, C.L. Brooks, D.R. Morgan, S. Krakowka, Essential Role of Urease in Pathogenesis of Gastritis Induced by *Helicobacter pylori* in Gnotobiotic Piglets, Infect. Immun. 59 (1991) 2470–2475.
- [11] K.A. Eaton, S. Krakowka, Effect of gastric pH on urease-dependent colonization of gnotobiotic piglets by *Helicobacter pylori*, Infect. Immun. 62 (1994) 3604–3607.
- [12] M. Campanale, E. Nucera, V. Ojetti, V. Cesario, T.A. Di Rienzo, G. D’Angelo, S. Pecere, F. Barbaro, G. Gigante, T. De Pasquale, A. Rizzi, G. Cammarota, D. Schiavino, F. Franceschi, A. Gasbarrini, Nickel free-diet enhances the *Helicobacter pylori* eradication rate: A pilot study, Dig. Dis. Sci. 59 (2014) 1851–1855.
<http://eutils.ncbi.nlm.nih.gov/entrez/eutils/elink.fcgi?dbfrom=pubmed&id=24595654>
&retmode=ref&cmd=prlinks.
- [13] M.J. Maroney, S. Ciurli, Nonredox nickel enzymes., Chem. Rev. 114 (2014) 4206–28.
doi:10.1021/cr4004488.
- [14] A. Merloni, O. Dobrovolska, B. Zambelli, F. Agostini, M. Bazzani, F. Musiani, S. Ciurli, Molecular landscape of the interaction between the urease accessory proteins UreE and UreG, Biochim. Biophys. Acta - Proteins Proteomics. 1844 (2014) 1662–1674.
doi:10.1016/j.bbapap.2014.06.016.
- [15] B. Zambelli, P. Turano, F. Musiani, P. Neyroz, S. Ciurli, Zn²⁺-linked dimerization of UreG from *Helicobacter pylori*, a chaperone involved in nickel trafficking and urease activation, Proteins Struct. Funct. Bioinforma. 74 (2009) 222–239.
doi:10.1002/prot.22205.
- [16] M. Bellucci, B. Zambelli, F. Musiani, P. Turano, S. Ciurli, *Helicobacter pylori* UreE, a urease accessory protein: specific Ni²⁺ - and Zn²⁺ -binding properties and interaction

- 1
2
3
553 with its cognate UreG, *Biochem. J.* 422 (2009) 91–100. doi:10.1042/BJ20090434.
5
554 [17] Y.H. Fong, H.C. Wong, M.H. Yuen, P.H. Lau, Y.W. Chen, K.-B. Wong, Structure of
8
555 UreG/UreF/UreH complex reveals how urease accessory proteins facilitate maturation
10
556 of *Helicobacter pylori* urease., *PLoS Biol.* 11 (2013) e1001678.
12
557 doi:10.1371/journal.pbio.1001678.
15
558 [18] B. Zambelli, A. Berardi, V. Martin-Diaconescu, L. Mazzei, F. Musiani, M.J. Maroney, S.
17
559 Ciurli, Nickel binding properties of *Helicobacter pylori* UreF, an accessory protein in the
18
560 nickel-based activation of urease, *J. Biol. Inorg. Chem.* 19 (2014) 319–334.
20
561 doi:10.1007/s00775-013-1068-3.
22
562 [19] J.H. Urban, J. Vogel, Translational control and target recognition by *Escherichia coli*
24
563 small RNAs in vivo, *Nucleic Acids Res.* 35 (2007) 1018–1037. doi:10.1093/nar/gkl1040.
26
564 [20] J. Bogomolovas, B. Simon, M. Sattler, G. Stier, Screening of fusion partners for high
28
565 yield expression and purification of bioactive viscotoxins., *Protein Expr. Purif.* 64 (2009)
30
566 16–23. doi:10.1016/j.pep.2008.10.003.
32
567 [21] N. Amar, A. Peretz, Y. Gerchman, A cheap, simple high throughput method for
34
568 screening native *Helicobacter pylori* urease inhibitors using a recombinant *Escherichia*
36
569 *coli*, its validation and demonstration of *Pistacia atlantica* methanolic extract effectivity
38
570 and specificity., *J. Microbiol. Methods.* 133 (2017) 40–45.
40
571 <http://linkinghub.elsevier.com/retrieve/pii/S0167701216303438>.
42
572 [22] M.J. Todd, J. Gomez, Enzyme kinetics determined using calorimetry: A general assay
44
573 for enzyme activity?, *Anal. Biochem.* 296 (2001) 179–187. doi:10.1006/abio.2001.5218.
46
574 [23] S. Benini, M. Cianci, L. Mazzei, S. Ciurli, Fluoride inhibition of *Sporosarcina pasteurii*
48
575 urease: structure and thermodynamics., *J. Biol. Inorg. Chem.* 19 (2014) 1243–61.
50
576 doi:10.1007/s00775-014-1182-x.
52
57
58
59
60
61
62
63
64
65

- 1
2
3
4
5
6
7
8
9
10
11
12
13
14
15
16
17
18
19
20
21
22
23
24
25
26
27
28
29
30
31
32
33
34
35
36
37
38
39
40
41
42
43
44
45
46
47
48
49
50
51
52
53
54
55
56
57
58
59
60
61
62
63
64
65
- [24] S. Benini, W.R. Rypniewski, K.S. Wilson, S. Mangani, S. Ciurli, Molecular details of urease inhibition by boric acid: insights into the catalytic mechanism., *J. Am. Chem. Soc.* 126 (2004) 3714–5. doi:10.1021/ja049618p.
- [25] B. Krajewska, Ureases I. Functional, catalytic and kinetic properties: A review, *J. Mol. Catal. B Enzym.* 59 (2009) 9–21. doi:10.1016/j.molcatb.2009.01.003.
- [26] M.A. Pearson, L.O. Michel, R.P. Hausinger, P.A. Karplus, Structures of Cys319 variants and acetohydroxamate-inhibited *Klebsiella aerogenes* urease, *Biochemistry.* 36 (1997) 8164–8172. doi:10.1021/bi970514j.
- [27] S. Benini, W.R. Rypniewski, K.S. Wilson, S. Miletta, S. Ciurli, S. Mangani, The complex of *Bacillus pasteurii* urease with acetohydroxamate anion from X-ray data at 1.55 Å resolution., *J. Biol. Inorg. Chem.* 5 (2000) 110–8. doi:10.1007/s007750050014.
- [28] N. Ha, S. Oh, J.Y. Sung, K.A. Cha, M.H. Lee, B. Oh, Supramolecular assembly and acid resistance of *Helicobacter pylori* urease, *Nat. Struct. Biol.* 8 (2001) 505–509. doi:10.1038/88563.
- [29] K. Phillips, D.J. Munster, R. a Allardyce, P.F. Bagshaw, Antibacterial action of the urease inhibitor acetohydroxamic acid on *Helicobacter pylori*., *J. Clin. Pathol.* 46 (1993) 372–373. doi:10.1136/jcp.46.4.372.
- [30] D.P. Griffith, M.J. Gleeson, H. Lee, R. Longuet, E. Deman, N. Earle, Randomized, double-blind trial of Lithostat (acetohydroxamic acid) in the palliative treatment of infection-induced urinary calculi., *Eur. Urol.* 20 (1991) 243–247.
- [31] N.C. Bailie, C.A. Osborne, J.R. Leininger, T.F. Fletcher, S.D. Johnston, P.N. Ogburn, D.P. Griffith, Teratogenic effect of acetohydroxamic acid in clinically normal Beagles, *Am. J. Vet. Res.* 47 (1986) 2604–2611.
- [32] A.J. Pope, C.D.N. Toseland, B. Rushant, S. Richardson, M. Mcvey, J. Hills, Effect of

- 1
2
3
4
5
6
7
8
9
10
11
12
13
14
15
16
17
18
19
20
21
22
23
24
25
26
27
28
29
30
31
32
33
34
35
36
37
38
39
40
41
42
43
44
45
46
47
48
49
50
51
52
53
54
55
56
57
58
59
60
61
62
63
64
65
- potent urease inhibitor, fluorofamide, on *Helicobacter* sp. in vivo and in vitro, *Dig. Dis. Sci.* 43 (1998) 109–119. doi:10.1023/A:1018884322973.
- [33] K. Macegoniuk, E. Grela, M. Biernat, M. Psurski, G. Gościński, A. Dzielak, A. Mucha, J. Wietrzyk, Ł. Berlicki, A. Grabowiecka, Aminophosphinates against *Helicobacter pylori* ureolysis-Biochemical and whole-cell inhibition characteristics., *PLoS One.* 12 (2017) e0182437. <http://journals.plos.org/plosone/article?id=10.1371/journal.pone.0182437>.
- [34] P. Kosikowska, Ł. Berlicki, Urease inhibitors as potential drugs for gastric and urinary tract infections: a patent review., *Expert Opin. Ther. Pat.* 21 (2011) 945–957. doi:10.1517/13543776.2011.574615.
- [35] L. Mazzei, M. Cianci, U. Contaldo, F. Musiani, S. Ciurli, Urease inhibition in the presence of N-(n-butyl)thiophosphoric triamide, a suicide substrate: structure and kinetics., *Biochemistry.* 56 (2017) 5391–5404. doi:10.1021/acs.biochem.7b00750.
- [36] L. Mazzei, M. Cianci, F. Musiani, S. Ciurli, Inactivation of urease by 1,4-benzoquinone: chemistry at the protein surface, *Dalt. Trans.* 45 (2016) 5455–5459. doi:10.1039/C6DT00652C.
- [37] Y. Sedan, O. Marcu, S. Lyskov, O. Schueler-Furman, Peptidrive server: derive peptide inhibitors from protein-protein interactions, *Nucleic Acids Res.* 44 (2016) W536–W541. doi:10.1093/nar/gkw385.
- [38] Y.H. Fong, H.C. Wong, C.P. Chuck, Y.W. Chen, H. Sun, K.B. Wong, Assembly of preactivation complex for urease maturation in *Helicobacter pylori*: Crystal structure of UreF-UreH protein complex, *J. Biol. Chem.* 286 (2011) 43241–43249. doi:10.1074/jbc.M111.296830.
- [39] R. Lam, V. Romanov, K. Johns, K.P. Battaile, J. Wu-Brown, J.L. Guthrie, R.P. Hausinger, E.F. Pai, N.Y. Chirgadze, Crystal structure of a truncated urease accessory

1
2
3
4
5
6
7
8
9
10
11
12
13
14
15
16
17
18
19
20
21
22
23
24
25
26
27
28
29
30
31
32
33
34
35
36
37
38
39
40
41
42
43
44
45
46
47
48
49
50
51
52
53
54
55
56
57
58
59
60
61
62
63
64
65

protein UreF from *Helicobacter pylori*, *Proteins Struct. Funct. Bioinforma.* 78 (2010) 2839–2848. doi:10.1002/prot.22802.

[40] P. Zhou, G. Wagner, Overcoming the solubility limit with solubility-enhancement tags: successful applications in biomolecular NMR studies., *J. Biomol. NMR.* 46 (2010) 23–31. doi:10.1007/s10858-009-9371-6.

[41] C. Follmer, Ureases as a target for the treatment of gastric and urinary infections, *J. Clin. Pathol.* 63 (2010) 424–430. doi:10.1136/jcp.2009.072595.

[42] K. Macegoniuk, E. Grela, J. Palus, E. Rudzińska-Szostak, A. Grabowiecka, M. Biernat, Ł. Berlicki, 1,2-Benzisoxaselenazol-3(2H)-one Derivatives As a New Class of Bacterial Urease Inhibitors., *J. Med. Chem.* 59 (2016) 8125–8133. <http://eutils.ncbi.nlm.nih.gov/entrez/eutils/elink.fcgi?dbfrom=pubmed&id=27524377&retmode=ref&cmd=prlinks>.

[43] L. Mazzei, V. Broll, S. Ciurli, An Evaluation of Maleic-Itaconic Copolymers as Urease Inhibitors, *Soil Sci. Soc. Am. J.* (2018). doi:10.2136/sssaj2017.09.0323.

[44] J.M. Bremner, Recent research on problems in the use of urea as a nitrogen fertilizer, *Fertil. Res.* 42 (1995) 321–329. doi:10.1007/BF00750524.

[45] M.J. Krogmeier, G.W. McCarty, J.M. Bremner, Potential phytotoxicity associated with the use of soil urease inhibitors, *Proc. Natl. Acad. Sci.* 86 (1989) 1110–1112. doi:10.1073/pnas.86.4.1110.

[46] C.J. Watson, H. Miller, Short-term effects of urea amended with the urease inhibitor N-(n-butyl) thiophosphoric triamide on perennial ryegrass, *Plant Soil.* 184 (1996) 33–45. doi:10.1007/BF00029272.

[47] E. Artola, S. Cruchaga, I. Ariz, J.F. Moran, M. Garnica, F. Houdusse, J.M.G. Mina, I. Irigoyen, B. Lasa, P.M. Aparicio-Tejo, Effect of N-(n-butyl) thiophosphoric triamide on

- 1
2
3
649 urea metabolism and the assimilation of ammonium by *Triticum aestivum* L, *Plant*
5
650 *Growth Regul.* 63 (2011) 73–79. doi:10.1007/s10725-010-9513-6.
8
651 [48] S. Cruchaga, E. Artola, B. Lasa, I. Ariz, I. Irigoyen, J.F. Moran, P.M. Aparicio-Tejo,
10
652 Short term physiological implications of NBPT application on the N metabolism of
11
653 *Pisum sativum* and *Spinacea oleracea*, *J. Plant Physiol.* 168 (2011) 329–336.
13
654 doi:10.1016/j.jplph.2010.07.024.
15
16
17
655 [49] L. Zanin, N. Tomasi, A. Zamboni, Z. Varanini, R. Pinton, The Urease Inhibitor NBPT
18
20
656 Negatively Affects DUR3-mediated Uptake and Assimilation of Urea in Maize Roots,
21
22
657 *Front. Plant Sci.* 6 (2015). doi:10.3389/fpls.2015.01007.
23
24
25
658 [50] L. Zanin, S. Venuti, N. Tomasi, A. Zamboni, R.M. De Brito Francisco, Z. Varanini, R.
26
27
659 Pinton, Short-Term Treatment with the Urease Inhibitor N-(n-Butyl) Thiophosphoric
28
30
660 Triamide (NBPT) Alters Urea Assimilation and Modulates Transcriptional Profiles of
31
32
661 Genes Involved in Primary and Secondary Metabolism in Maize Seedlings, *Front. Plant*
33
34
662 *Sci.* 7 (2016). doi:10.3389/fpls.2016.00845.
35
36
37
663 [51] X. Yang, M. Koochi-Moghadam, R. Wang, Y.Y. Chang, P.C.Y. Woo, J. Wang, H. Li, H.
38
39
664 Sun, Metallochaperone UreG serves as a new target for design of urease inhibitor: A
40
42
665 novel strategy for development of antimicrobials, *PLoS Biol.* 16 (2018).
43
44
666 doi:10.1371/journal.pbio.2003887.
45
46
47
667 [52] C. Sheng, G. Dong, Z. Miao, W. Zhang, W. Wang, State-of-the-art strategies for
48
49
668 targeting protein-protein interactions by small-molecule inhibitors., *Chem. Soc. Rev.* 44
50
51
669 (2015) 8238–8259. <http://xlink.rsc.org/?DOI=C5CS00252D>.
52
53
54
670 [53] N. London, B. Raveh, D. Movshovitz-Attias, O. Schueler-Furman, Can self-inhibitory
55
56
671 peptides be derived from the interfaces of globular protein-protein interactions?,
57
58
672 *Proteins Struct. Funct. Bioinforma.* 78 (2010) 3140–3149. doi:10.1002/prot.22785.
59
60
61
62
63
64
65

- 1
2
3
4
5
6
7
8
9
10
11
12
13
14
15
16
17
18
19
20
21
22
23
24
25
26
27
28
29
30
31
32
33
34
35
36
37
38
39
40
41
42
43
44
45
46
47
48
49
50
51
52
53
54
55
56
57
58
59
60
61
62
63
64
65
- [54] G.T. Heller, F.A. Aprile, M. Vendruscolo, Methods of probing the interactions between small molecules and disordered proteins., *Cell. Mol. Life Sci.* 74 (2017) 3225–3243. <http://link.springer.com/10.1007/s00018-017-2563-4>.
- [55] V.N. Uversky, Intrinsic disorder-based protein interactions and their modulators., *Curr. Pharm. Des.* 19 (2013) 4191–4213. <http://eutils.ncbi.nlm.nih.gov/entrez/eutils/elink.fcgi?dbfrom=pubmed&id=23170892&retmode=ref&cmd=prlinks>.
- [56] F. Biagi, F. Musiani, S. Ciurli, Structure of the UreD-UreF-UreG-UreE complex in *Helicobacter pylori*: A model study, *J. Biol. Inorg. Chem.* 18 (2013) 571–577. doi:10.1007/s00775-013-1002-8.
- [57] F. Musiani, D. Gioia, M. Masetti, F. Falchi, A. Cavalli, M. Recanatini, S. Ciurli, Protein Tunnels: The Case of Urease Accessory Proteins, *J. Chem. Theory Comput.* 13 (2017) 2322–2331. doi:10.1021/acs.jctc.7b00042.
- [58] D.A. Bonsor, E.J. Sundberg, Dissecting protein-protein interactions using directed evolution, *Biochemistry.* 50 (2011) 2394–2402. <http://pubs.acs.org/doi/abs/10.1021/bi102019c>.
- [59] K.E. Beenken, P.M. Dunman, F. McAleese, D. Macapagal, E. Murphy, S.J. Projan, J.S. Blevins, M.S. Smeltzer, Global gene expression in *Staphylococcus aureus* biofilms., *J Bacteriol.* 186 (2004) 4665–4684. <http://eutils.ncbi.nlm.nih.gov/entrez/eutils/elink.fcgi?dbfrom=pubmed&id=15231800&retmode=ref&cmd=prlinks>.
- [60] M. Müsken, S. Di Fiore, A. Dötsch, R. Fischer, S. Häussler, Genetic determinants of *Pseudomonas aeruginosa* biofilm establishment., *Microbiol. (Reading, Engl).* 156 (2010) 431–441.

1
2
3
4
5
6
7
8
9
10
11
12
13
14
15
16
17
18
19
20
21
22
23
24
25
26
27
28
29
30
31
32
33
34
35
36
37
38
39
40
41
42
43
44
45
46
47
48
49
50
51
52
53
54
55
56
57
58
59
60
61
62
63
64
65

[http://eutils.ncbi.nlm.nih.gov/entrez/eutils/elink.fcgi?dbfrom=pubmed&id=19850623
&retmode=ref&cmd=prlinks.](http://eutils.ncbi.nlm.nih.gov/entrez/eutils/elink.fcgi?dbfrom=pubmed&id=19850623&retmode=ref&cmd=prlinks)

- [61] B.D. Jones, C. V. Lockett, D.E. Johnson, J.W. Warren, H.L.T. Mobley, Construction of a urease-negative mutant of *Proteus mirabilis*: Analysis of virulence in a mouse model of ascending urinary tract infection, *Infect. Immun.* 58 (1990) 1120–1123.
- [62] S. Gattermann, R. Marre, Cloning and expression of *Staphylococcus saprophyticus* urease gene sequences in *Staphylococcus carnosus* and contribution of the enzyme to virulence, *Infect. Immun.* 57 (1989) 2998–3002.
- [63] J. V. Ligon, G.E. Kenny, Virulence of ureaplasma urease for mice, *Infect. Immun.* 59 (1991) 1170–1171.